Aging of di-isopropyl-phosphorylated human butyrylcholinesterase

Patrick MASSON*[1], Pierre-Louis FORTIER†, Christine ALBARET†, Marie-Thérèse FROMENT*, Cynthia F. BARTELS‡ and Oksana LOCKRIDGE‡

*Centre de Recherches du Service de Santé des Armées, Unité de Biochimie, 24 avenue des Maquis du Grésivaudan, B.P. 87, 38702 La Tronche Cédex, France, †Centre d'Études du Bouchet, DGA, B.P. 3, 91710 Vert-le-Petit, France, and ‡University of Nebraska Medical Center, Eppley Institute, 600 South 42nd Street, Omaha, NE 68198-6805, U.S.A.

Organophosphate-inhibited cholinesterases can be reactivated by nucleophilic compounds. Sometimes phosphylated (phosphorylated or phosphonylated) cholinesterases become progressively refractory to reactivation; this can result from different reactions. The most frequent process, termed 'aging', involves the dealkylation of an alkoxy group on the phosphyl moiety through a carbocation mechanism. In attempting to determine the amino acid residues involved in the aging of butyrylcholinesterase (BuChE), the human BuChE gene was mutated at several positions corresponding to residues located at the rim of the active site gorge and in the vicinity of the active site. Mutant enzymes were expressed in Chinese hamster ovary cells. Wild-type BuChE and mutants were inhibited by di-isopropyl fluorophosphate at pH 8.0 and 25 °C. Di-isopropyl-phosphorylated enzymes were incubated with the nucleophilic oxime 2-pyridine aldoxime methiodide and their reactivatability was determined. Reactivatability was expressed by the first-order rate constant of aging and/or the half-life of aging ($t_{\frac{1}{2}}$). The $t_{\frac{1}{2}}$ was found to be of the order of 60 min for wild-type BuChE. Mutations on Glu-197 increased $t_{\frac{1}{2}}$ 60-fold. Mutation W82A increased $t_{\frac{1}{2}}$ 13-fold. Mutation D70G increased $t_{\frac{1}{2}}$ 8-fold. Mutations in the vicinity of the active site serine residue had either moderate or no effect on aging; $t_{\frac{1}{2}}$ was doubled for F329C and F329A, increased only 4-fold for the double mutant A328G + F329S, and no change was observed for the A328G mutant, indicating that the isopropoxy chain to be dealkylated does not directly interact with Ala-328 and Phe-329. These results were interpreted by molecular modelling of di-isopropyl-phosphorylated wild-type and mutant enzymes. Molecular dynamics simulations indicated that the isopropyl chain that is lost interacted with Trp-82, suggesting that Trp-82 has a role in stabilizing the carbonium ion that is released in the dealkylation step. This study emphasized the important role of the Glu-197 carboxylate in stabilizing the developing carbocation, and the allosteric control of the dealkylation reaction by Asp-70. Indeed, although Asp-70 does not interact with the phosphoryl moiety, mutation D70G affects the rate of aging. This indirect control was interpreted in terms of change in the conformational state of Trp-82 owing to internal motions of the Ω loop (Cys-65–Cys-92) in the mutant enzyme.

INTRODUCTION

Organophosphates are potent inhibitors of cholinesterases [acetylcholinesterase (AChE; EC 3.1.1.7) and butyrylcholinesterase (BuChE; EC 3.1.1.8)]; most of these compounds are used as insecticides, pesticides or drugs [1]. The most toxic organophosphates are chemical warfare agents [2]. The progressive inhibition of cholinesterases by organophosphates is due to phosphylation (phosphorylation or phosphonylation) of their active site serine Ser-198 (200) in human (Hu) BuChE [3]. Phosphylated cholinesterases react very slowly with water; they can be reactivated only by strong nucleophilic compounds such as oximes, which are used as antidotes against organophosphorus poisoning [1,4,5]. Organophosphoryl adducts can undergo dealkylation of an alkoxy group, which converts phosphylated cholinesterases into non-reactivatable species, described as 'aged'. Aging is a first-order process [6] that has been found to depend on the nature of the enzyme (BuChEs tend to age more rapidly than AChEs), the nature and stereochemistry of the organophosphate and the physicochemical conditions of the medium [7–9].

The generally accepted mechanism for the dealkylation reaction proposed by Michel et al. [10] involves a transient carbocation. This can result from protonation of the alkoxy oxygen [11], leading to scission of the C–O bond and formation of the carbonium ion and of a negatively charged monophosphylate ester of serine, i.e. the aged enzyme [12–14]. This reaction can be depicted as in Scheme 1, where (a) is the free enzyme, (b) the organophosphate, (c) the covalent phosphyl adduct that can be reactivated by oximes, (d) the developing carbonium intermediate, (e) the dealkylation products (R-OH, R-derived alkenes) resulting from the release of the carbonium ion into the medium (propan-2-ol is the major product when the organophosphate is di-isopropyl fluorophosphate (DFP) [15]) and (f) the monophosphylate ester of serine [16]. Recently, a 'push–pull' mechanism of carbocation formation, involving both the glutamic residue (Glu-*199*) adjacent to the active site serine and the catalytic histidine residue (His-*440*) was proposed [17,18]. According to this mechanism, (1) formation of the carbocation is promoted by the strong negative electrostatic field of Glu-*199* and (2) protonated His-*440* acts as an acid catalyst for the cleavage of the C–O bond. Molecular dynamics calculations indicate that the anionic monophosphylate ester is stabilized by hydrogen bond interactions with water and oxyanion hole residues and electrostatic interaction with protonated His-*440*.

The importance of protonated catalytic histidine (protonated

Abbreviations used: AChE, acetylcholinesterase; *BCHE*, butyrylcholinesterase gene, BuChE, butyrylcholinesterase; DFP, di-isopropyl fluorophosphate; DIP, di-isopropylphosphoryl; Hu, human; 2-PAM, 2-pyridinealdoxime methiodide. Note that italicized numbers refer to the amino acid residues in *Torpedo* AChE that correspond to BuChE or AChE residues.

[1] To whom correspondence should be addressed.

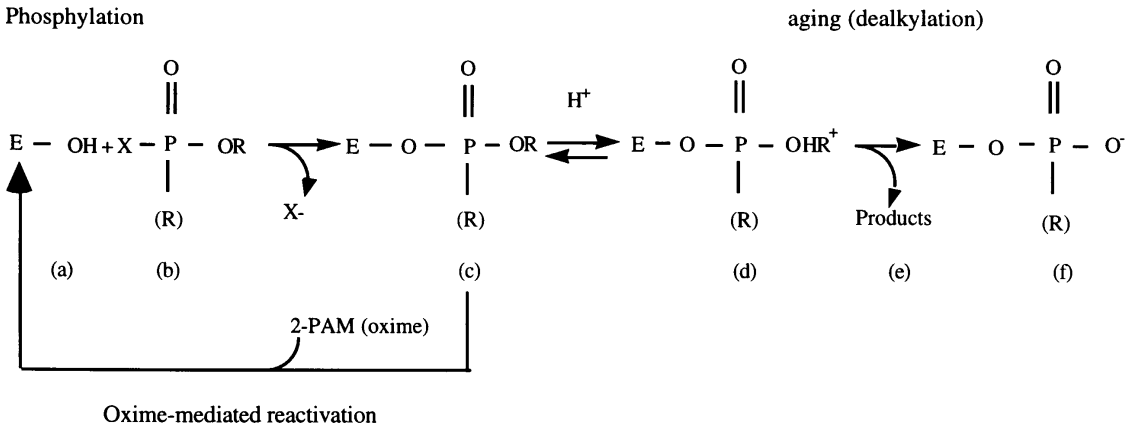

Scheme 1 The mechanism of cholinesterase phosphylation and dealkylation of the phosphylated enzyme

His-*440*) in the aging process of both AChE and BuChE has long been recognized from pH-dependence studies [9,11] and from the observation that there is no aging when histidine is labelled by diethyl pyrocarbonate [15,19]. Several other active site residues involved in the dealkylation of soman-phosphonylated AChE have been identified [20–22]. In AChE, formation of the carbonium ion seems to be promoted by the glutamic carboxylate next to the phosphylated serine residue (Ser-*199*) [17,20,22]. Other residues in the active centre have also been found to have a role in aging, including hydrogen-bond network residues Glu-450 (*443*), Tyr-133 (*130*) and Glu-202 (*199*) as well as Phe-338 (*331*) and Trp-86 (*84*) in HuAChE [22]. In both HuAChE [22] and HuBuChE [23] the aspartic residue located at the rim of the active site cleft (Asp-*72*) was found to be involved in the control of the aging process.

The molecular basis for the resistance to reactivation of aged cholinesterases may be ascribed partly to the electrostatic repulsion of oximate by the negatively charged oxygen of the P–O^- group and the adjacent negatively charged Glu-*199* [18]. It also originates in conformational changes, concomitant with the dealkylation reaction, at the enzyme active-site gorge. Several works showed that aging is associated with cholinesterase conformational change [14,24] and increase in conformational stability [25–28]. This might result from the formation of a salt bridge between catalytic protonated histidine and the negatively charged oxygen atom on the monophosphylate moiety. Evidence for a salt bridge in the stabilization of aged BuChE is the pK of 8.5–9 as estimated from differential scanning calorimetry of native and soman-aged BuChE at different pH values ([28], and P. Masson, J. Clément, S. Rey and C. Cléry, unpublished work).

To determine the amino acids involved in the aging process, we expressed selected mutants of HuBuChE and determined their aging rate constants after phosphorylation by DFP. Mutations of Glu-197, mutation of the residue expected to interact with an alkoxy chain (Trp-82) and mutation of Asp-70 located at the rim of the active site cleft were all found to slow the aging rate process. To understand the effects of mutations, a molecular modelling study of the phosphorylated enzyme and its mutants was performed. Such an approach has proved to be very powerful in probing the active site of AChE by molecular dynamics of its non-aged soman adducts [29]. The present study revealed that mutations of Glu-197 had no drastic effect on the local structure of the non-aged adduct, so that the role of Glu-197 was not to maintain structure. Instead these results underlined the crucial role of the negative charge on Glu-197 in the dealkylation process. The residue belonging to the choline-binding site (Trp-82) was found to interact, mainly through van der Waals contacts, with an isopropyl chain of DFP. In particular, molecular dynamics of phosphorylated wild-type BuChE showed a stacking of the aromatic ring of Trp-82 against the putative leaving isopropoxy group. This stacking was not observed in the simulation of the phosphorylated D70G mutant adduct, since the Ω loop of BuChE underwent a conformational change resulting in a shift of Trp-82 relative to the isopropoxy group. Thus our results show that aging of DFP-phosphorylated BuChE involves amino acid residues equivalent to those promoting aging of soman-phosphonylated AChE, Trp-82 and Glu-197; moreover our results demonstrate that the remote Asp-70 exerts an indirect control on the aging process.

MATERIALS AND METHODS

Chemicals

DFP was purchased from Sigma Chemical Co. (St. Louis, MO, U.S.A.) and 2-pyridinealdoxime methiodide (2-PAM) was from Ega-Chemie (Steinteim, Germany). Racemic soman (pinacolyl methylphosphonofluoridate) was obtained from the Centre d'Études du Bouchet (Vert-le-Petit, France). Other chemicals were of biochemical grade. A stock solution of 10 mM DFP in anhydrous methanol acidified by 0.01 % acetic acid was stored at −30 °C in borosilicate tubes.

Mutagenesis and expression of HuBuChE

Site-directed mutagenesis of the HuBuChE gene (*BCHE*) cDNA was performed with PCR and *Pfu* DNA polymerase as described [30]. Mutated residues were Asp-70 (*72*), Trp-82 (*84*), Glu-197 (*199*), Ala-328 (*330*) and Phe-329 (*331*). Single and double mutants were made. Mutations of residues Asp-70, Trp-82 and Glu-197 were expected to slow the aging process. Mutations of residues Ala-328 and Phe-329 were made to test the possibility that the leaving isopropyl chain interacted with these residues. Eleven mutants were studied: A70G, W82A, E197D, E197Q, E197G, A328G, F329A, F329C, F329S, A328G+F329S and E197Q+F329S.

Recombinant wild-type and mutant BuChEs were expressed in stably transfected Chinese hamster ovary K1 cells as previously described [30].

Purification of recombinant BuChE mutants

Recombinant enzymes were partly purified by affinity chromatography on a procainamide–Sepharose column [30], dialysed to remove procainamide and concurrently concentrated in an Amicon stirred cell with a PM10 membrane and stored at +4 °C in sterile 20 mM phosphate buffer, pH 7.0, containing 1 mM EDTA.

Enzyme activity measurements

BuChE activity was assayed with the Ellman method [31] with butyrylthiocholine iodide (1 mM) as substrate in 0.1 M sodium phosphate, pH 7.0, at 25 °C. Units of activity are μmol of butyrylthiocholine hydrolysed/min.

Enzyme phosphorylation and measurement of aging rates

Wild-type and mutant enzymes in 50 mM sodium phosphate, pH 8.0 (2–2.5 ml of approx. 0.2 unit/ml, i.e. max. 9 pmol of active sites) were inhibited to 90–95 % by 30 μl of 20–100 μM DFP in methanol at 25 °C. The final methanol concentration (less than 2 %, v/v) had no significant effect on enzyme activity. After enzyme had been inhibited, aliquots were removed at various times after inhibition (from 5 min to 7 days) and immediately incubated with 2-PAM (1 or 10 mM) in the same buffer at 25 °C. The time courses of reactivation were followed by measuring the activity recovered as a function of time of incubation with 2-PAM. Reactivation curves reached a plateau corresponding to maximally reactivated enzyme in approx. 5 h. The height of the plateau was not changed at 24 h. Reactivated enzyme activity was therefore measured after 24 h of incubation with 2-PAM. It should be noted that the dilution factor of reactivated enzyme in the Ellman assay was 1:150; under these conditions, 2-PAM, which is a competitive inhibitor (e.g. K_i = 0.20 mM for wild-type and K_i = 3.10 mM for D70G) of BuChE-catalysed hydrolysis of butyrylthiocholine [23], did not significantly affect K_m and thus did not interfere with activity measurements. Each experiment was done at least six times. The aging rates of wild-type and W82A soman adducts were determined in a similar way.

The rate constant of aging (k_a) was determined from [32]:

$$\log[100(E_r - E_i)/(E_0 - E_i)] = -k_a t \quad (1)$$

where E_0 is the activity of control enzyme in the presence of 2-PAM, E_i is the residual activity after inhibition by DFP, E_r is the activity of reactivated enzyme and t is the time after inhibition by DFP and before the addition of 2-PAM. Results were also expressed as half-lives of aging: $t_{\frac{1}{2}} = \ln(2/k_a)$.

Molecular modelling and dynamics

The three-dimensional model of wild-type HuBuChE used as the starting structure was the Harel model [33]. All calculations were performed on an SGI Power Indigo 2 workstation and an SGI Power Challenge 4xR8000 super computer. Cartesian coordinates for BuChE were kindly provided by Dr. Harel [33]. Hydrogen atoms were added in INSIGHT 95.0 (Biosym, San Diego, CA, U.S.A.). All Arg, Lys, Asp, Glu, N-terminal and C-terminal groups were ionized except Glu-441, which is located in a hydrophobic environment. The missing fragment 482–486 was added by using the standard Biosym library; optimization of its geometry was achieved in DISCOVER 2.9 (Biosym). Minimization was performed with 200 steepest-descent steps followed by 200 conjugate-gradient steps while constraining all heavy atoms of the structure to their original positions [constant of 100 kcal/mol (418 kJ/mol)]. For mutants, replacement of the wild-type residue was achieved before minimization and the mutated residue was not constrained during the calculation. In a second step, Ser-198 was phosphorylated by DFP and His-438 was protonated. Charges for the phosphorylated serine residue were derived from calculations *ab initio* with the program DMol 2.3.5 (Biosym). The phosphoryl oxygen of DFP was placed in the vicinity of the oxyanion hole (Gly-116, Gly-117 and Ala-199). A grid on isopropyl torsion angles was then performed in QUANTA 96 (Molecular Simulations, Cambridge, U.K.) to minimize the electronic and steric interactions of isopropyl chains with the binding pocket. Finally, minimization was achieved by 500 steepest-descent steps followed by 500 adopted basis Newton–Raphson steps constraining all protein heavy atoms outside a shell of 20 Å from the phosphorylated serine [constant force of 40 kcal/mol (167 kJ/mol) between 20 and 22 Å, and 80 kcal/mol (335 kJ/mol) above 22 Å) with the molecular mechanics program CHARMM 23.2 [34].

Stochastic boundary molecular dynamics (SBMD) runs [35] were performed on DFP-phosphorylated wild-type and D70G mutant BuChE with a parallel version of the software CHARMM 23.2 (Molecular Simulations) [34]. The all-hydrogen model was used and water was represented by the TIP3P type [36]. For non-bond interactions, a cut-off of 11 Å was applied with a switching function between 8 and 10 Å. The dielectric constant was set to 1. The reaction region was defined by a 23 Å sphere centred on the Cα atom of residue Ile-69. A buffer region was made of a 2 Å layer surrounding the reaction region. The remaining atoms of the protein constituted the reservoir region. The Cα of residue Ile-69 was chosen to include all the Ω loop atoms in the reaction region during the simulations. All non-hydrogen atoms of the protein in the buffer region were harmonically constrained with a boundary force. We used the simplified Debye–Waller factor values of Nakagawa et al. [37] in our calculations. The force was weighted by a switching function that decreased from 0.5 to 0 when moving from the buffer/reservoir boundary to the reaction region [35]. Solvation of the active site was achieved by using a pre-equilibrated sphere (25 Å radius) centred on the Cα atom of residue Ile-69. Water molecules overlapping the adduct (cut-off of 2.8 Å) were deleted. Four successive rotations of this sphere were applied, to minimize the remaining holes in the covalent complex. For the solvent boundary forces, a radial distribution function centred on the Cα of residue Ile-69 was applied to the oxygen atoms [38]. The frictional coefficients related to the stochastic forces were assigned as follows: 62 ps for the heavy atoms in the protein and 200 ps for water oxygens [35,38]. SHAKE [39] was used to constrain bonds with hydrogen atoms, allowing a 2 fs time step. The SBMD simulation was performed by equilibrating the system at 300 K for 20 ps for each enzyme. Production dynamics of 200 and 800 ps were performed for non-aged phosphorylated wild-type and D70G mutant enzymes respectively. Coordinates were saved every 0.5 ps in each dynamics simulation.

RESULTS AND DISCUSSION

Aging of di-isopropylphosphoryl (DIP) wild-type BuChE

To slow the aging process, inhibition of BuChE by DFP was performed at pH 8.0 and 25 °C [9]. The half-life of aging of the wild-type enzyme was found to be 60 min (Table 1). This value is consistent with $t_{\frac{1}{2}}$ = 28 min reported by Hobbiger [40] for aging of human plasma BuChE at pH 7.8 and 37 °C and $t_{\frac{1}{2}}$ = 3 h in water at 24 °C [16] for horse BuChE.

Table 1 Rate constant (k_a) and half-life of aging ($t_{\frac{1}{2}}$) of DFP-phosphorylated wild-type BuChE and mutants in 50 mM sodium phosphate, pH 8.0, at 25 °C

Results are means ± S.E.M. for at least six independent determinations.

Enzyme	$10^5 k_a$ (min)	$t_{\frac{1}{2}}$ (min)	$t_{\frac{1}{2}}$ ratio, mutant to wild-type
Wild-type	1130 ± 30	60 ± 5*	1
D70G	140 ± 30	490 ± 80	8.0 ± 1.3
W82A	85	~ 810†	13†
E197D	190 ± 50	360 ± 100	5.8 ± 4.5
E197Q	20 ± 4	3650 ± 650	60 ± 40
E197G	7.3 ± 0.9	9500 ± 1100	155 ± 30
A328G	1310 ± 140	53 ± 2	0.9 ± 0.1
F329C	570 ± 20	120 ± 2	2.0 ± 0.2
F329A	580 ± 50	120 ± 10	2.0 ± 0.3
F329S	460 ± 60	150 ± 11	2.5 ± 0.3
A328G + F329S	265 ± 10	260 ± 7.0	4.2 ± 0.4
E197Q + F329S	21 ± 3	3300 ± 400	54 ± 10.7

* $t_{\frac{1}{2}} = 12$ min at pH 6.8 and 25 °C by using the pH-stat method with butyrylcholine chloride as substrate (P. Masson and M. Th. Froment, unpublished work).

† $t_{\frac{1}{2}} = 13.5$ h with racemic soman instead of $t_{\frac{1}{2}} = 9$ min for wild-type enzyme; ratio ≈ 90.

Effect of mutations on aging of DIP BuChE

Mutations of residues located in different areas of the active site cleft were found to affect the rate constant of aging of DFP-phosphorylated BuChE. As seen in Table 1, the most significant alterations were observed for mutations of residue Glu-197. Aging was slowed up to 155 times in the E197G mutant. Glu-197 has been found to stabilize the developing carbocation in soman-phosphonylated AChE [20–22]. Mutation W82A decreased the rate of the aging process with DFP to 1/15, and decreased the rate of aging with soman to 1/90 from $t_{\frac{1}{2}} = 9$ min for wild-type BuChE to $t_{\frac{1}{2}} = 800$ min for the W82A mutant enzyme. The effect of the W82A mutation in BuChE was far less pronounced than the effect of the corresponding mutation in HuAChE (W86A), where the soman-phosphonylated enzyme aged at less than 1/1000 of the rate of the wild-type enzyme [22]. Mutation D70G caused a decrease to one-eighth in the rate constant of aging. In contrast, mutations F329C, F329A and F329S had little effect on the aging reaction. This is another noteworthy difference from HuAChE, in which the mutation F338A, equivalent to the F329A mutation of BuChE, decreased the rate of aging of soman-phosphonylated adduct to 1/80 of the wild-type rate [22]. For soman-phosphonylated AChE it has been proposed that Phe-338 (*331*) is involved in the dealkylation reaction by stabilization of the catalytic His-447 (*440*) via charge–π interactions [22]. The *BCHE* single mutation A328G had no effect at all on dealkylation or aging, indicating that the isopropoxy chains of DIP do not interact directly with residues Ala-328 and Phe-329.

Molecular modelling and molecular dynamics simulations

Role of residues in the vicinity of the active site

Unlike soman, whose bulky pinacoloxy chain interacts with Trp-82, the O-alkoxy chain (isopropoxy) of DFP cannot fill the whole 'anionic' subsite of BuChE. In particular, no interaction of the isopropyl chain R_1 with Trp-82 was observed in the minimized structure of the wild-type DFP-phosphorylated enzyme (Figure 1, top panel). However, mutation W82A was found to decrease the rate of aging. We therefore performed a molecular dynamics simulation of this adduct to see whether a conformational change in the indole ring of Trp-82 could explain the biochemical data. During a 200 ps trajectory, the aromatic ring of Trp-82 was found to stack against the isopropyl chain R_1 making close van der Waals contacts with the methyl groups (Figure 1, bottom panel). The conformational transition of Trp-82 arose from the disruption of the H-bond between Hϵ2 of Trp-82 indole ring and the hydroxy oxygen of Tyr-440, allowing the Trp-82 side chain to rotate closer to R_1. Interestingly, the second isopropyl chain (R_2) at the bottom of the active site was found to stack against Trp-231, leading to the sandwich-like structure depicted in Figure 1 (bottom panel). We believe that the effect of Trp-82 on the aging process originates in the stacking of the indole ring on the leaving alkoxy chain. In this position Trp-82 could polarize the O–C_1 bond or, most probably, stabilize the developing cation through interactions with the π electrons of the indole ring. Such interactions might also take place in the case of the soman-BuChE adduct, its aging process being faster than that of the DFP-BuChE adduct ($t_{\frac{1}{2}} = 9$ min instead of 60 min) owing to a stronger inductive effect of the more substituted pinacolyl moiety. The 10-fold difference in half-life between soman-phosphonylated W82A-BuChE ($t_{\frac{1}{2}} = 800$ min) and W86A-AChE ($t_{\frac{1}{2}} = 7000$ min) might, in contrast, result from additional interactions in the 'anionic' site of AChE that do not exist in the active site of BuChE.

The structural transition of Trp-82 did not affect the interaction of the phosphoryl oxygen with the oxyanion hole, nor did it change the distances to the three amide hydrogens of Gly-116, Gly-117 and Gly-199, which remained in an accepted range for such hydrogen bonds (see the time series in Figure 2). As expected, the strong hydrogen bond formed between Hϵ2 of His-438 and the adjacent alkoxy oxygen during the minimization (see Figure 1) was found to remain during the time course of the dynamics (Figure 2), supporting the mechanism described in Scheme 1.

Concerning the acidic residue Glu-197, one of the side chain carboxylic oxygens is in the vicinity of carbon C-1 of the DIP moiety (average distance 4.47 Å). In addition, the carboxy oxygen of Glu-197 was found to interact directly with residue Glu-441 through a hydrogen bond with the hydroxy hydrogen of this non-charged residue (Figure 3). Though it has been shown for HuAChE [21] that the corresponding two residues are bridged by a water molecule, we found a direct interaction. This direct interaction was very effective in maintaining Glu-197 close to the isopropoxy chain (R_1) to be dealkylated in the simulation of the DIP-BuChE adduct. Because the side chain of Glu-197 is located near the centre of the active site in a region free of overlapping protein atoms, mutation of Glu-197 to an aspartate, glutamine or glycine residue did not lead to drastic conformational changes in the minimized structures of the phosphorylated mutant enzymes. These observations confirm that, as with AChE, Glu-197 mediates the aging process through its negative charge by stabilizing the carbonium ion [17,20]. Moreover, the fact that the E197D mutation caused a decrease to one-sixth in the rate of aging relative to that of wild-type BuChE underlines the role of the Glu-197 side chain, whose size allows the carboxylate to be suitably placed for stabilizing the carbocation.

We compared the final structure obtained by molecular dynamics calculations with that of the minimized soman-HuAChE adduct [22]. No important changes were found regarding the position of the catalytic His-438 (His-447 in HuAChE) with respect to the neighbouring Phe-329 (Phe-338 in HuAChE) in both adducts. Because we were unable to observe a meaningful decrease in the half-life of aging of DIP-BuChE for the F329A mutant, stabilization of the imidazolium ring of His-438 through a charge–π interaction with Phe-329 seems ques-

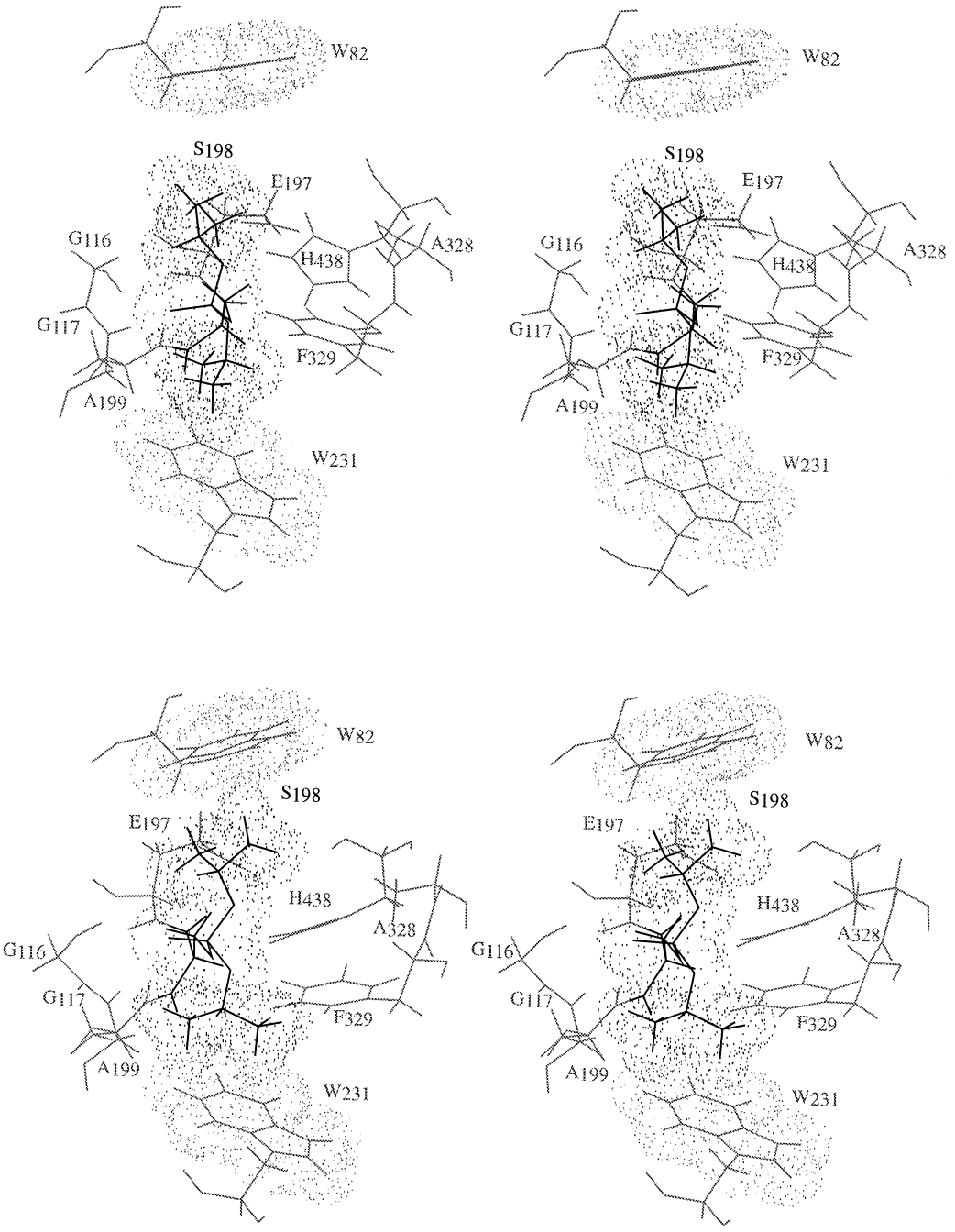

Figure 1 Stereo views of the wild-type BuChE active site in which Ser-198 is covalently attached to DIP

Van der Waals surfaces for side chains of residues Trp-82, Trp-231 and the phosphorylated serine are represented. The adducts are non-aged, that is, both isopropyl groups of DIP are present. The top panel shows the energy-minimized structure. The phosphoryl oxygen-binding pocket (oxyanion hole) is 9 Å away from the Trp-82 ring, preventing any interaction between the isopropyl chain R_1 and Trp-82, even in the most favourable orientation. The bottom panel gives the final structure of the 200 ps molecular dynamics simulation of the adduct, showing stacking of R_1 against Trp-82.

tionable. It is difficult to reach a conclusion on this point because the leaving alkyl chains of soman (pinacolyl) and DFP (isopropyl) are different in size. Nevertheless, no specific interactions between the R_1 isopropyl chain of DFP and Phe-329 could be observed in the energy-minimized structure of the DIP-BuChE conjugate, although we observed that the methyl moiety bound to the asymmetric carbon of the pinacolyl moiety pointed towards Phe-338 in the soman-HuAChE adduct. Thus van der Waals contact between this methyl and Phe-338 in the soman-HuAChE adduct might contribute to the formation of the carbocation.

Role of Asp-70 at the rim of the active site cleft

A puzzling question is how Asp-70 affects the rate of aging. A tentative explanation might involve the conformational state of the Ω loop. This loop, located between Cys-65 (*67*) and Cys-92

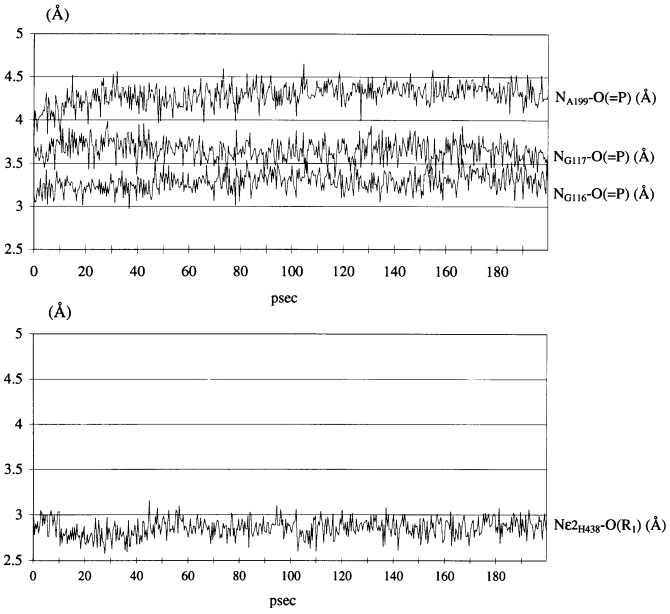

Figure 2 Time series for the distances between the phosphoryl oxygen of DIP and the nitrogen atoms of the oxyanion hole (Gly-116, Gly117 and Ala-199), and between Nε2 of His-438 and the alkoxy oxygen of R_1

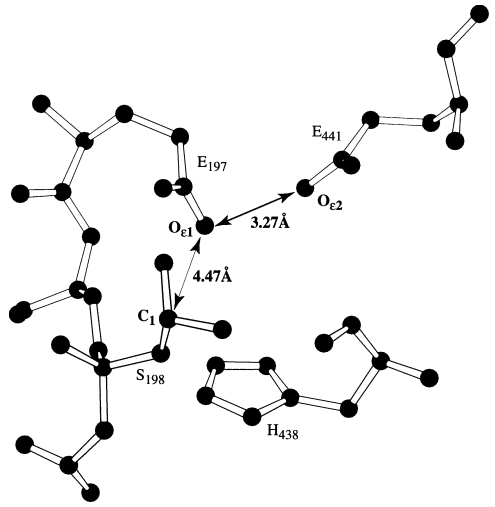

Figure 3 Close-up of the average structure of the 200 ps dynamics showing the relative positions of residues Glu-197, His-438, Glu-441 and the phosphorylated Ser-198

C_1 is a carbon in the R_1 isopropoxy group of DIP. The carboxylic oxygen $O_{\varepsilon1}$ of Glu-197 interacts with C_1 and with the uncharged hydroxy oxygen $O_{\varepsilon2}$ of Glu-441.

(*94*), has been shown to be involved in the allosteric modulation of AChE by peripheral anionic site ligands [41]. To test whether such an allosteric modulation could occur in aging reaction, we performed an 800 ps molecular dynamics simulation of D70G mutant bound to DIP. Despite the length of this run, we were unable to observe large conformational changes in the loop. Residues belonging to the Ω loop showed similar root-mean-square (RMS) fluctuations in the dynamics of both the wild-type and mutant enzyme adducts (Figure 4). However, disruption of the H-bond between Asp-70 carboxylate and Tyr-332 was found

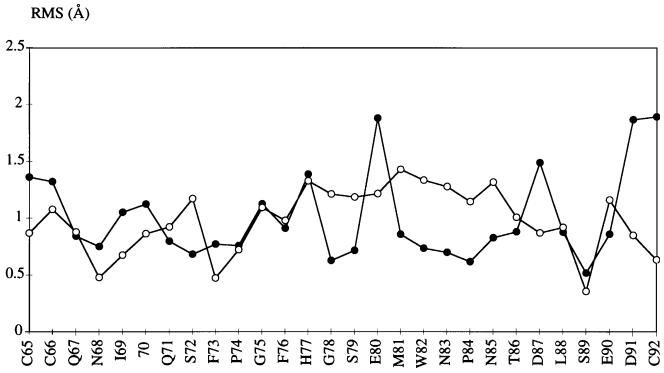

Figure 4 Root-mean-square (RMS) fluctuations of the Ω loop residues (backbone atoms) for the simulation of the phosphorylated wild-type enzyme (○) and for the first 200 ps dynamics of the phosphorylated D70G mutant (●)

to affect the motion of the 70–77 segment, which underwent a slight displacement during the first few picoseconds of the simulation. This displacement induced a conformational change in Trp-82, whose indole ring shifted from its original position, moving away from the R_1 isopropyl group and thus preventing the indole–isopropyl interaction in the D70G mutant. This could explain the slower (one-eighth) rate of aging of the DIP-D70G enzyme. Figure 5 compares the average structures of the dynamics of wild-type and D70G mutant adducts in this region of the enzyme structure. As can be seen, the global motion of the loop in the D70G mutant cannot be analysed in terms of lid opening as it can for *Candida rugosa* lipase [42]. Indeed, it has recently been shown that mutations of different residues in the Ω loop of AChE barely affected the catalytic properties of the enzyme [43]. As a consequence, allosteric modulation of the enzyme activity by the Ω loop would implicate small conformational transitions

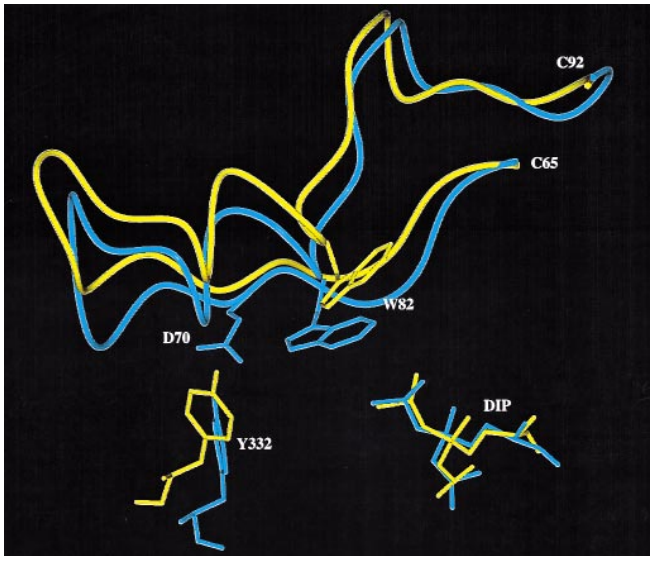

Figure 5 Average conformation of the Ω loop in the two dynamics simulations: phosphorylated wild-type enzyme (blue), and phosphorylated D70G mutant (yellow)

Note the shift in position of Trp-82.

rather than large distortions in this region of the enzyme structure [44].

Conclusion and prospects

The single mutants E197G and E197Q and the double mutant E197Q+F329S enzymes, which have very slow aging rate constants, could be of biotechnological interest as bioscavengers for decontamination and detoxification or as parts of biosensors for organophosphate detection. Other double mutants, e.g. D70G+E197G, in association with oximes could be of pharmacological interest as pseudocatalytic scavengers against organophosphate poisoning. The behaviour of the D70G mutant enzyme also raises the question of the relevance of the D70G mutation in people because this is a natural mutation. The plasma of individuals homozygous for the D70G *BCHE* allele contains what is called 'atypical' BuChE [45]. 'Atypical' BuChE has no known natural physiological disadvantage but does drastically prolong apnoea in patients treated with muscle relaxants such as succinylcholine or mivacurium. Because the aging rate of the D70G mutant enzyme is lower than that of the wild-type enzyme, the efficacy of oximes in treatment of organophosphate poisoning is expected to be slightly improved in people possessing 'atypical' BuChE because the long-term reactivatable plasma enzyme will function as an endogeneous pseudocatalytic organophosphate scavenger.

We thank Dr. A. Shafferman for the coordinates of the modelled structure of somanphosphonylated HuAChE. This work was supported by the Direction de la Recherche et de la Technologie grants DRET 94/05 and 96/12 to P.M. and by the U.S. Medical Research and Material Command under grant DAMD 17-94-J-4005 to O.L.

REFERENCES

1 Ballantyne, B. and Marrs, T. C. (1992) Clinical and Experimental Toxicology of Organophosphates and Carbamates, Butterworth–Heinemann, Oxford
2 Marrs, T. C., Maynard, R. L. and Sidell, F. R. (1996) Chemical Warfare Agents, John Wiley, Chichester
3 Main, A. R. (1979) Pharmacol. Ther. **6**, 579–628
4 Worek, F., Kirchner, T., Bäker, M. and Szinicz, L. (1996) Arch. Toxicol. **70**, 497–503
5 Dawson, R. M. (1994) J. Appl. Toxicol. **14**, 317–331
6 Davies, D. R. and Green, A. L. (1956) Biochem. J. **63**, 530–535
7 Karczmar, A. G., Usdin, E. and Wills, J. H. (1970) International Encyclopedia of Pharmacology and Therapeutics: Anticholinesterase Agents, pp. 249–262. Pergamon Press, Oxford
8 Aldridge, W. N. and Reiner, E. (1972) Enzyme Inhibitors as Substrates, pp. 79–90, North-Holland, Amsterdam
9 Keijer, J. H., Wolring, G. Z. and DeJong, L. P. A. (1974) Biochim. Biophys. Acta **334**, 145–155
10 Michel, H. O., Hackley, B. E., Berkowitz, L., List, G., Hackley, E. B., Gillilan, W. and Pankau, M. (1967) Arch. Biochem. Biophys. **121**, 29–34
11 Benschop, H. P. and Keijer, J. H. (1966) Biochim. Biophys. Acta **128**, 586–588
12 Gunwald, J., Segall, Y., Shirin, E., Waysbort, D., Steinberg, N., Silman, I. and Ashani, Y. (1989) Biochem. Pharmacol. **38**, 3157–3168
13 Segall, Y., Waysbort, D., Barak, D., Ariel, N., Doctor, B. P., Grunwald, J. and Ashani, Y. (1993) Biochemistry **32**, 13441–13450
14 Steinberg, N., Van der Drift, A. C. M., Grunwald, J., Segall, Y., Shirin, E., Haas, E., Ashani, Y. and Silman, I. (1989) Biochemistry **28**, 1248–1253
15 Beauregard, G., Lum, J. and Roufogalis, B. D. (1981) Biochem. Pharmacol. **30**, 2915–2920
16 Berends, F., Posthumus, C. H., Sluys, I. V. and Deierkauf, F. A. (1959) Biochim. Biophys. Acta **34**, 576–578
17 Qian, N. and Kovach, I. M. (1993) FEBS Lett. **336**, 263–266
18 Bencsura, A., Enyedy, I. and Kovach, I. M. (1995) Biochemistry **34**, 8989–8999
19 Masson, P., Marnot, B. and Morelis, P. (1984) Trav. Sci. Serv. Sante Armées Fr. **5**, 234-235
20 Saxena, A., Doctor, B. P., Maxwell, D. M., Lenz, D. E., Radic, Z. and Taylor, P. (1993) Biochem. Biophys. Res. Commun. **197**, 343–349
21 Ordentlich, A., Kronman, C., Barak, D., Stein, D., Ariel, N., Marcus, D., Velan, B. and Shafferman, A. (1993) FEBS Lett. **334**, 215–220
22 Shafferman, A., Ordentlich, A., Barak, D., Stein, D., Ariel, N. and Velan, B. (1996) Biochem. J. **318**, 833–840
23 Masson, P., Froment, M. T., Bartels, C. F. and Lockridge, O. (1997) Biochem. J. **325**, 53–61
24 Amitai, G., Ashani, Y., Gafni, A. and Silman, I. (1982) Biochemistry **21**, 2060–2069
25 Masson, P. and Goasdoué, J. L. (1986) Biochim. Biophys. Acta **869**, 304–313
26 Ashani, Y., Gentry, M. K. and Doctor, B. P. (1990) Biochemistry **29**, 2456–2463
27 Masson, P., Gouet, P. and Cléry, C. (1994) J. Mol. Biol. **238**, 466–478
28 Masson, P., Rey, S., Cléry, C., Fontaine, N., Kronman, C., Velan, B. and Shafferman, A. (1997) in Proc. 1996 Medical Defense Bioscience Review (King, J. M., ed.), pp. 43–52, U.S. Army Medical Research and Materiel Command, Aberdeen PG, MD
29 Bencsura, A., Enyedy, I. Y. and Kovach, I. M. (1996) J. Am. Chem. Soc. **118**, 8531–8541
30 Lockridge, O., Blong, R. M., Masson, P., Froment, M. T., Millard, C. B. and Broomfield, C. (1997) Biochemistry **36**, 786–795
31 Ellman, G. L., Courtney, K. D., Andres, V. and Featherstone, R. M. (1961) Biochem. Pharmacol. **7**, 88–95
32 Heilbronn, E. (1963) Biochem. Pharmacol. **12**, 25–36
33 Harel, M., Sussman, J. L., Krejci, E., Bon, S., Chanal, P., Massoulié, J. and Silman, I. (1992) Proc. Natl. Acad. Sci. U.S.A. **89**, 10827–10831
34 Brooks, B. R., Bruccoleri, R. E., Olafson, B. D., States, D. J., Swaminathan, S. and Karplus, M. (1983) J. Comput. Chem. **4**, 187–217
35 Brooks, III, C. L., Brünger, A. and Karplus, M. (1985) Biopolymers **24**, 843–865
36 Jorgensen, W. L., Chandrasekhar, J., Madura, J. D., Impey, R. W. and Klein, M. L. (1983) J. Chem. Phys. **79**, 926–935
37 Nakagawa, S., Yu, H.-A., Karplus, M. and Umeyama, H. (1993) Proteins Struct. Funct. Genet. **16**, 172–194
38 Brünger, A. T., Brooks, III, C. L. and Karplus, M. (1984) Chem. Phys. Lett. **105**, 495–500
39 Rickaert, J.-P., Ciccotti, G. and Berendsen, H. J. C. (1977) J. Comput. Phys. **23**, 327–341
40 Hobbiger, F. (1955) Br. J. Pharmacol. **10**, 356–362
41 Barak, D., Ordentlich, A., Bromberg, A., Kronman, C., Marcus, C., Lazar, A., Ariel, N., Velan, B. and Shafferman, A. (1995) Biochemistry **34**, 15444–15452
42 Grochulski, P., Li, Y., Schrag, J. D. and Cygler, M. (1994) Protein Sci. **3**, 82–91
43 Faerman, C., Ripoll, D., Bon, S., Le Feuvre, Y., Morel, N., Massoulié, J., Sussman, J. L. and Silman, I. (1996) FEBS Lett. **386**, 65–71
44 Velan, B., Barak, D., Ariel, N., Leitner, M., Bino, T., Ordentlich, A. and Shafferman, A. (1996) FEBS Lett. **395**, 22–28
45 Lockridge, O. (1990) Pharmacol. Ther. **47**, 35–60

Received 2 January 1997/1 May 1997; accepted 24 June 1997